

# Fluorescent Zn<sup>II</sup> Chemosensor Mediated by a 1,8-Naphthyridine Derivative and Its Photophysical Properties

Wenxiu Luo,<sup>[a]</sup> Mengjiao Liu,<sup>[a]</sup> Ting Yang,<sup>[a]</sup> Xia Yang,<sup>[a]</sup> Yi Wang,<sup>\*,[a]</sup> and Haifeng Xiang<sup>\*,[b]</sup>

One of the greatest challenges in using fluorescent chemosensors for highly selective and sensitive transition-metal ions is finding an efficient and simple method for its synthesis. In this study, a highly efficient fluorescence chemosensor for Zn<sup>II</sup> was developed from *N*-Boc-*L*-proline modified 1,8-naphthyridine. The fluorescence intensity of the chemosensor was increased significantly only in the presence of Zn<sup>II</sup> ion which provided a perceived color change for rapid visual sensing, while other metal ions showed fluorescence quenching or little changes. It

was worth noting that the chemosensor **L** distinguished Zn<sup>II</sup> from Cd<sup>II</sup> commonly having similar properties. The solvent effect and possible bonding mode for fluorescence enhancement have been also discussed. Results of this study indicated that the Boc-group in *L*-proline significantly improved the sensitivity and selectivity for Zn<sup>II</sup> detection performance, as confirmed by comparison experiments and time dependent-density functional theory (TD-DFT) calculations.

## 1. Introduction

Owing to the attractive properties of high sensitivity, low cost, and straightforward operation, fluorescent chemosensors have enjoyed popularity as an ideal tool to detect the presence of transition-metal ions and anions.<sup>[1]</sup> In this respect, exploitation of chemical sensors for copper, iron, cobalt, and zinc ions are especially important, because they are the fundamental elements of the biological systems.<sup>[2]</sup> Among them, the development of methods to detect Zn<sup>II</sup> has received great attention, owing to its environmental and biological significance.<sup>[3]</sup> Zn<sup>II</sup> is the second most abundant of transition-metal ions in living organisms after iron ions. Compounds of Zn play an important role in numerous cellular metabolisms such as gene expression, regulation of metalloenzymes, apoptosis, and co-factors of neurotransmission catalysis.<sup>[4]</sup> Disorder of Zn<sup>II</sup> metabolism is not only offensive to environmental ecology, but can also damage the human nervous system. Parkinson's disease, Alzheimer's disease, and epilepsy have been reportedly associated with an imbalance of Zn<sup>II</sup> in the body.<sup>[5]</sup> For these reasons, a va-

riety of fluorescent chemosensors, including di-2-picolyamine (DPA), quinoline, bipyridine, acyclic polyamines, iminodiacetic acid, triazole, and schiff-base, have been developed for the detection of Zn<sup>II</sup>.<sup>[6]</sup> However, most of them suffer from interference of some transition-metal ions. For a Zn<sup>II</sup> chemosensor, Cd<sup>II</sup> often exhibits similar fluorescence responses with Zn<sup>II</sup> and consequently has a serious interference in Zn<sup>II</sup> detection. Thus, the quest for novel Zn<sup>II</sup>-selective chemosensors, which are not affected by other transition-metal ions, particularly Cd<sup>II</sup>, are of considerable significance.<sup>[7]</sup>

Although many commercial Zn<sup>II</sup> chemosensors have been developed, the design and synthesis of new ones with high sensitivity, selectivity, and reliability to satisfy various needs remains challenging. 1,8-Naphthyridine is a well-known nitrogen ligand. The nitrogen atom in 1,8-naphthyridine demonstrates a strong affinity for many transition-metal ions and, thus, the preparation and photophysical properties of many ligands and complexes based on 1,8-naphthyridine have been reported.<sup>[8]</sup> However, amino-acid-modified 1,8-naphthyridine compounds are rarely reported, and there are only limited examples of 1,8-naphthyridine derivatives for fluorescent metal-ion sensing applications.<sup>[9]</sup>

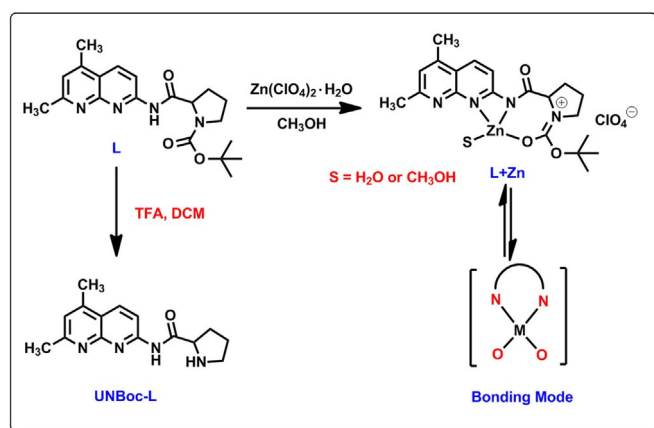
In this paper, we report a simple, cost-efficient chemosensor based on an *N*-Boc(*tert*-butyloxy carbonyl)-protected *L*-proline-modified 1,8-naphthyridine derivative (**L**) for the trace detection of Zn<sup>II</sup> (Scheme 1). *L*-Proline derivatives have featured during the last 10 years as readily available and cheap catalysts, which have been used in various transformations with good yields.<sup>[10]</sup> The introduction of an additional carbonyl binding site in *L*-proline would help to change the coordination numbers of the 1,8-naphthyridine ligand edifice, which might lead to a stronger coordination ability with particular metal ions with high sensitivity and selectivity. To the best of our knowledge, this observation has not been described. The se-

[a] W. Luo, M. Liu, T. Yang, X. Yang, Dr. Y. Wang  
College of Chemistry and Materials Science  
Sichuan Normal University  
Chengdu, 610068 (P.R. China)  
E-mail: wangyi@sicnu.edu.cn

[b] Dr. H. Xiang  
College of Chemistry, Sichuan University  
Chengdu, 610041 (P.R. China)  
E-mail: xianghaifeng@scu.edu.cn

Supporting Information and the ORCID identification number(s) for the author(s) of this article can be found under:  
<https://doi.org/10.1002/open.201800083>.

© 2018 The Authors. Published by Wiley-VCH Verlag GmbH & Co. KGaA. This is an open access article under the terms of the Creative Commons Attribution-NonCommercial-NoDerivs License, which permits use and distribution in any medium, provided the original work is properly cited, the use is non-commercial and no modifications or adaptations are made.



Scheme 1. Proposed bonding mode of L and L + Zn<sup>II</sup>.

lective sensing capability of L for zinc ions over a wide range of competing cations, with respect to bonding mode and chelation mechanism, has also been highlighted and discussed.

## 2. Results and Discussion

### 2.1. Effect of Solvents

It is well known that solvents play very important role in the preparation of organometallic complexes. The binding ability and sensing performance of a ligand with the same metal cation can be diverse in different solvents. The UV/Vis absorption (Figure S1) and fluorescence spectra (Figure 1) of L ( $1 \times 10^{-5}$  M) changed obviously in the presence of various solvents. The protic property and polarity of CH<sub>3</sub>OH have a significant impact on the fluorescence enhancement and binding ability of L with Zn<sup>II</sup>. It was clear that a significant fluorescence enhancement was found in CH<sub>3</sub>OH solution upon addition of Zn<sup>II</sup>. Therefore, CH<sub>3</sub>OH was selected as an appropriate solvent to study the performance of probe L with Zn<sup>II</sup>.

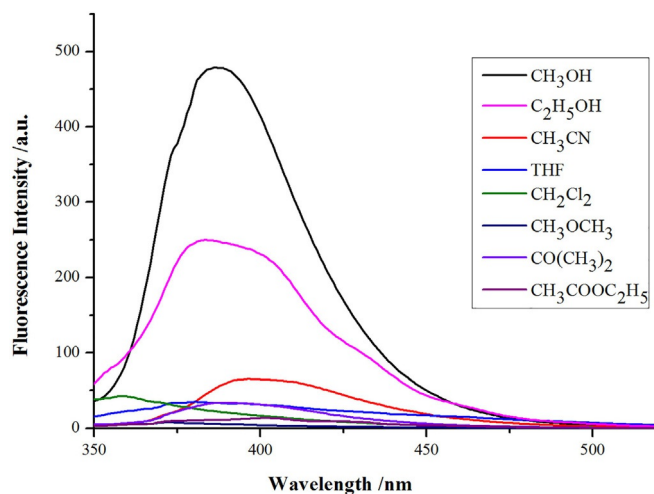


Figure 1. The fluorescence of L (10 μM) in various solvents at  $\lambda_{\text{ex}} = 349$  nm.

### 2.2. Effect of Metal Ions

The binding and sensing ability of L with different metal ions, including Li<sup>I</sup>, K<sup>I</sup>, Mn<sup>II</sup>, Mg<sup>II</sup>, Cu<sup>II</sup>, Zn<sup>II</sup>, Cd<sup>II</sup>, Hg<sup>II</sup>, Pb<sup>II</sup>, Fe<sup>III</sup>, Fe<sup>II</sup>, Cr<sup>III</sup>, Ni<sup>II</sup>, Ag<sup>I</sup>, and Co<sup>II</sup> were checked in CH<sub>3</sub>OH at room temperature. As shown as Figure 2, fluorescence spectra of L demonstrated

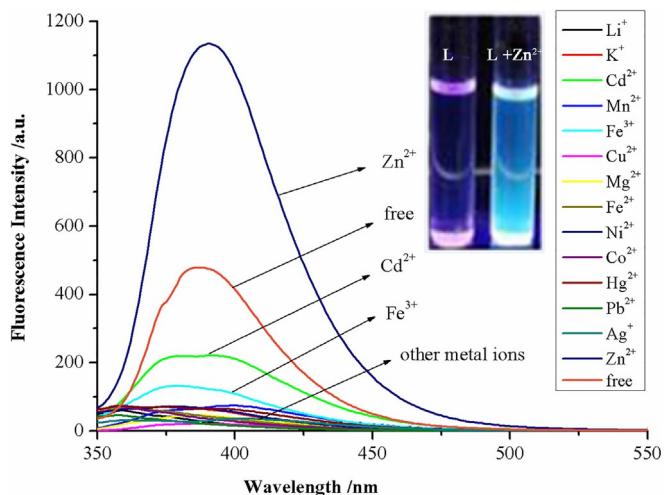
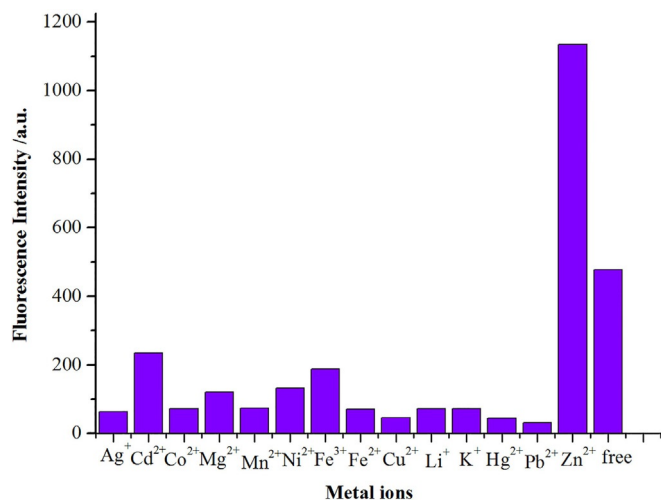


Figure 2. Fluorescence emission spectra of L (10 μM) in the presence of different metal ions (300 μM) in CH<sub>3</sub>OH. Excitation at  $\lambda_{\text{ex}} = 349$  nm.

drastic changes in the presence of different metal ions. As soon as Zn<sup>II</sup> was added, the fluorescence peak red-shifted to approximately 400 nm with a 2.5-fold enhancement of fluorescence intensity. Conversely, a large excess of other metal ions induced fluorescence quenching or little change. Interestingly, only upon addition of Zn<sup>II</sup> was a variation in emission colors observed, from dark purple to light blue, which could even be detected by the naked-eye (Figure 2). These results clearly indicate that L showed a selective detection for Zn<sup>II</sup>. The fluorescence enhancement may be attributed to the chelation-enhanced fluorescence phenomenon (CHEF),<sup>[11]</sup> owing to the fact that 1,8-naphthyridine in combination with carboxamide linkages –C(O)NH– could act as a chelation agent and could easily form stable Zn<sup>II</sup> complexes. The addition of Zn<sup>II</sup> increased the fluorescence intensity steadily at 388 nm. Therefore, it was believed that the existence of zinc ions in the solution promotes the dissociation of protons, consequently resulting in the formation of complexes.

The affinity toward one metal ion in solution is one of the most important characteristics for a chemosensor. As shown as Figure 3, the fluorescence intensity was enhanced with the addition of Zn<sup>II</sup>. This effect was not observed with the addition of other metal ions like alkali metals K<sup>I</sup> and Li<sup>I</sup>, alkaline earth metal Mg<sup>II</sup>, and other transition-metal ions Mn<sup>II</sup>, Cu<sup>II</sup>, Zn<sup>II</sup>, Cd<sup>II</sup>, Hg<sup>II</sup>, Pb<sup>II</sup>, Fe<sup>III</sup>, Fe<sup>II</sup>, Cr<sup>III</sup>, Ni<sup>II</sup>, Ag<sup>I</sup>, and Co<sup>II</sup>, even at very high concentrations (300 μM). This indicated that L had good selectivity toward Zn<sup>II</sup>.

Next, to investigate the practicability of L as a selective fluorescent chemosensor for Zn<sup>II</sup>, the competitive experiments were carried out in the absence or presence of different metal



**Figure 3.** Fluorescence intensity profile changes of **L** (10  $\mu\text{M}$ ) in the absence and presence of 300  $\mu\text{M}$  of various metal ions in  $\text{CH}_3\text{OH}$  solution at room temperature.

ions. The changes in fluorescence enhancement of **L** in the presence of  $\text{Zn}^{\text{II}}$  and other metal ions are shown in the histogram in Figure 4. The results demonstrated that the response of **L** to  $\text{Zn}^{\text{II}}$  remained almost unaffected, even in the presence of 1 equivalent of  $\text{Zn}^{\text{II}}$  mixed with 30 equivalents of the other metal ions. It was notable that the sensitivity of **L** for  $\text{Zn}^{\text{II}}$  remained unchanged without disturbances from  $\text{Cd}^{\text{II}}$ , despite the fact that  $\text{Zn}^{\text{II}}$  and  $\text{Cd}^{\text{II}}$  are part of the IIB group and share analogous chemical properties. Thus, when they appear together in the solution, it is difficult for a chemosensor to distinguish between them. These results certified that **L** could be used as a selective sensor for  $\text{Zn}^{\text{II}}$ , especially for resolution of  $\text{Zn}^{\text{II}}$  from  $\text{Cd}^{\text{II}}$ . Additional studies showed that the binding of **L** to  $\text{Zn}^{\text{II}}$  was not affected by high concentrations of  $\text{Cu}^{\text{II}}$  and  $\text{Ni}^{\text{II}}$ , which are generally known to be strong fluorescence inhibitors.<sup>[12]</sup>

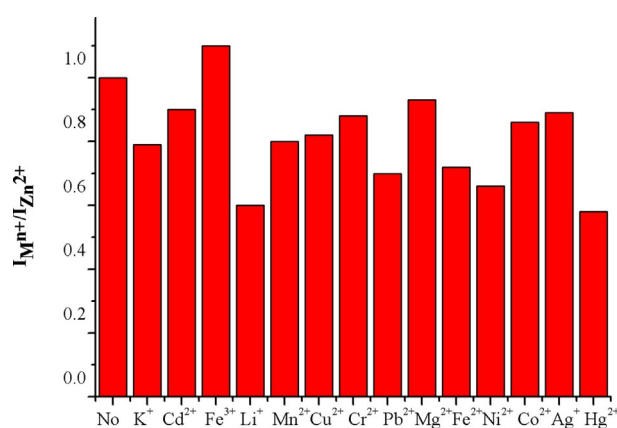


**Figure 4.** Fluorescent response of **L** (10  $\mu\text{M}$ ) with 1 equivalent of  $\text{Zn}^{\text{II}}$  + 30 equivalents of different other metal ions at  $\lambda_{\text{em}} = 388 \text{ nm}$ .

### 2.3. Binding Mode of **L** with $\text{Zn}^{\text{II}}$

The fluorescence titration experiments were performed by adding different quantities of zinc ions to a solution of **L** with a constant concentration (10  $\mu\text{M}$ ). The emission intensity increased gradually upon the addition of  $\text{Zn}^{\text{II}}$  (Figure 5). The fluo-

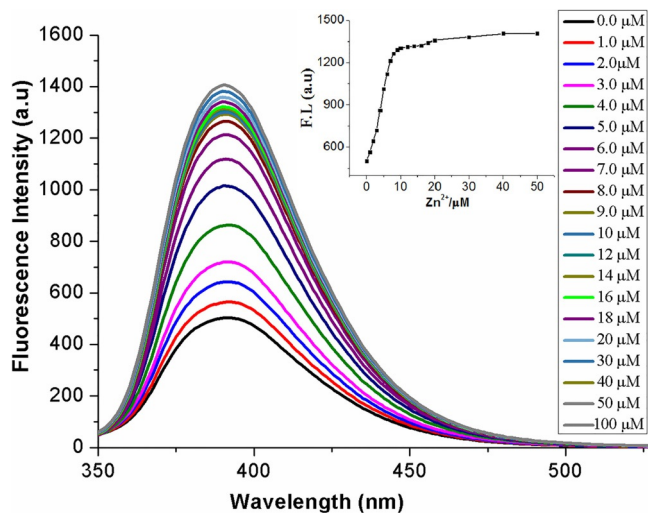


**Figure 5.** Concentration-dependent fluorescence enhancement of **L** (10  $\mu\text{M}$ ) on the addition of various amounts of  $\text{Zn}^{\text{II}}$  (0–100 equiv) in  $\text{CH}_3\text{OH}$ .

rescence emission at 388 nm was saturated after 1 equivalent of  $\text{Zn}^{\text{II}}$  and no further distinct changes were subsequently observed. This phenomenon indicated that the stoichiometry of the **L**+ $\text{Zn}^{\text{II}}$  complex was 1:1. Fluorescence titration experiments showed that the dissociation constant ( $K$ ) of the **L**+ $\text{Zn}^{\text{II}}$  complex was  $5.94 \times 10^4 \text{ M}^{-1}$  (Figure S2). This value was comparable to those of reported  $\text{Zn}^{\text{II}}$  chemosensors ( $10$  to  $10^7$ ).<sup>[2c]</sup> The detection limits of **L** for the analysis of  $\text{Zn}^{\text{II}}$  was calculated to be  $3.4 \times 10^{-6} \text{ M}$  on the basis of  $3\sigma/k$  (where  $\sigma$  is the standard deviation). It indicated that **L** was satisfactory for the detection of  $\text{Zn}^{\text{II}}$  to hygienic standards for drinking water, within the defined limits (China, GB5749-2006,  $1 \text{ mg L}^{-1}$ ). Furthermore, the fluorescence emission intensity was saturated when the  $\text{Zn}^{\text{II}}$  molar fraction reached 0.5. The Job's plots for the **L**+ $\text{Zn}^{\text{II}}$  complex also revealed 1:1 complexation stoichiometry (Figure S3).

To elucidate the fluorescence behaviors of the chemosensor **L** and its **L**+ $\text{Zn}^{\text{II}}$  complex, IR experiments were carried out. The IR spectrum of **L** showed a broad absorption peak in a range of  $3329$ – $3670 \text{ cm}^{-1}$  and a characteristic peak at  $2976 \text{ cm}^{-1}$ , which were assigned to the stretching vibrations of N–H in the amide region and a C–H stretch. Sharp peaks at  $1686$  and  $1604 \text{ cm}^{-1}$  were assigned to the stretching vibrations of carboxyl functionality in the amide and ester in *tert*-butyl carboxylate group (Boc) unit of *L*-proline, respectively. Additionally, a series of peaks at  $1513$ – $1124 \text{ cm}^{-1}$  implied the presence of C=N pyridyl groups in 1,8-naphthyridine (Figure S4). Upon addition of one equivalent of  $\text{Zn}^{\text{II}}$ , the C=O peak at  $1604 \text{ cm}^{-1}$  of the Boc unit disappeared, indicating the ester of C=O had coordinated with the Zn ion and converted to a C–O–M bond (Figure S5). New peaks appeared at  $629$  and

1085  $\text{cm}^{-1}$  with strong signals, which were assigned to special spectrum of O–M and  $\text{CH}_3\text{OH}$ .<sup>[13]</sup> These variations in spectrum signals showed the existence of  $\text{CH}_3\text{OH}$ , which was likely to bond with  $\text{Zn}^{\text{II}}$  to yield a four-coordinated complex (Scheme 1). Indeed, such a typical tetrahedral ONNO geometry is beneficial for the stability of  $\text{Zn}^{\text{II}}$  complexes.<sup>[14]</sup>  $^1\text{H}$  NMR spectroscopy in  $\text{CD}_3\text{OD}$  was also studied (Figure S10). In the presence of  $\text{Zn}^{\text{II}}$ , the protons of the carboxamide group at 8.91 ppm disappeared, owing to deprotonation. The protons of 1,8-naphthyridine and the pyrrole moiety were shifted downfield. Thus, we propose that the carboxamide N and the carboxyl O atoms might coordinate to the  $\text{Zn}^{\text{II}}$ .

To further interpret the influence of the Boc unit of *L*-proline in the reaction of **L** with  $\text{Zn}^{\text{II}}$ , we synthesized a similar *L*-proline-modified 1,8-naphthyridine ligand (**UNBoc-L**, Scheme 1) to investigate its fluorescence changes upon addition of a wide range of metal ions under the same conditions as **L** (Figure S11). Conversely, adding many metal ions, including  $\text{Pb}^{\text{II}}$ ,  $\text{Zn}^{\text{II}}$ , and  $\text{Ni}^{\text{II}}$ , to **UNBoc-L** solution led to a significant enhancement or decrease in the fluorescence intensity, which indicated that **UNBoc-L** had an inferior selectivity than **L**. Therefore, the Boc unit of **L** was proven to have an important role for the efficient and selective detection of  $\text{Zn}^{\text{II}}$ .

## 2.4. Orbital Energy Calculations by TD-DFT

The binding properties of **L** and the importance of the carboxyl binding site of the Boc group toward  $\text{Zn}^{\text{II}}$  were further verified by theoretical calculations. As shown in Figure 6, the natu-

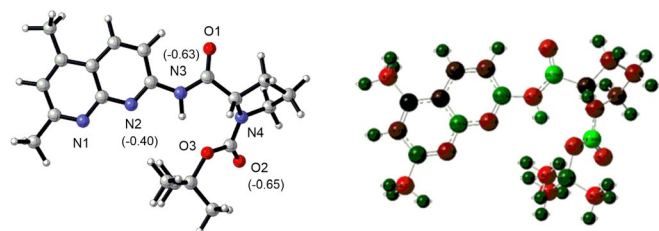


Figure 6. Optimized structure and the NBO atomic charges of **L**.

ral bond orbital (NBO) negative charge density of N2, N3, and O2 were  $-0.403$ ,  $-0.63$ , and  $-0.65$  respectively, indicating a strong coordination ability for positive metal ions. The coordinating atoms of N2, N3, and O2 reacted with  $\text{Zn}^{\text{II}}$  to yield a seven-membered and a four-membered ring, respectively (Scheme 1). Another coordinated oxygen atom came from the solvent,  $\text{CH}_3\text{OH}$ . According to the results above, we speculated that a four-coordinated single-nuclear complex between **L** and  $\text{Zn}^{\text{II}}$  was a reasonable binding mode. Based on the experimental results and NBO charge density calculations, we proposed that the high selectivity and sensitivity of the presently developed chemosensor **L** towards  $\text{Zn}^{\text{II}}$  could be described as follows. Carboxamide derivatives have been employed as a chelating agent to form stable  $\text{Zn}^{\text{II}}$  complexes, as investigated by Amirnasr et al.<sup>[11b]</sup> In chemosensor **L**, large electron density accumulation on the carboxyl oxygen adjacent to pyrrole facili-

tates the formation of an enol conformer upon chelation with  $\text{Zn}^{\text{II}}$ . Upon the formation of a stable cyclic four-coordinated complex with  $\text{Zn}^{\text{II}}$ , the rigidity of the molecular edifice increased, leading to fluorescence enhancement.

To understand more on the photophysical property of the free host and its metal complex in this system, we calculated possible spectral assignments of **L** and **L**+ $\text{Zn}^{\text{II}}$  complexes in the ground and excited states (Figure 7). In ligand **L**, the elec-

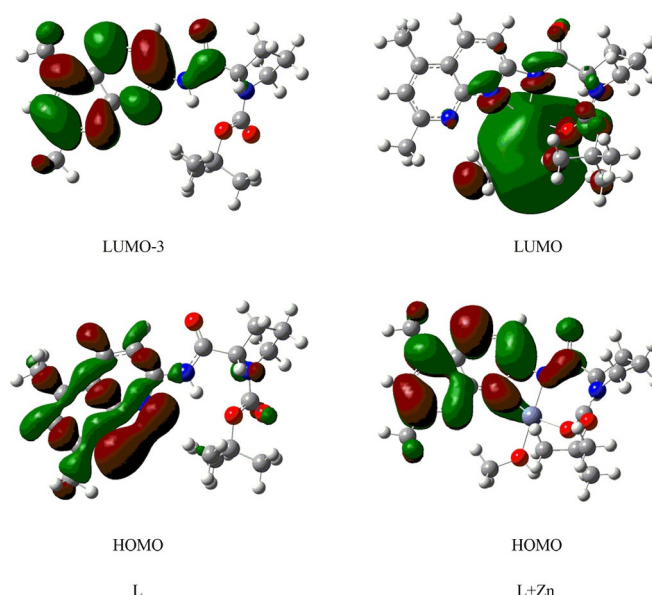


Figure 7. Frontier molecular orbitals of **L** and **L**+ $\text{Zn}^{\text{II}}$  relevant to the fluorescence enhancement.

tron density was primarily distributed over the naphthyridine group, both in the highest occupied molecular orbital (HOMO) and the lowest unoccupied molecular orbital (LUMO). The lowest-energy transition of **L** comes from the HOMO-3 to LUMO orbital transitions (64%). In the **L**+ $\text{Zn}^{\text{II}}$  complex, the electron density remained distributed over the naphthyridine group in the HOMO, whereas the electron density was distributed over the  $\text{Zn}^{\text{II}}$  in the LUMO. The lowest-energy transition of **L**+ $\text{Zn}^{\text{II}}$  comes from the HOMO to LUMO orbital transitions (100%). The calculation results proved that ligand-to-metal charge transfer (LMCT) process and CHEF phenomenon occurred in the excited states of the **L**+ $\text{Zn}^{\text{II}}$  complex. This LMCT from the excited naphthyridine moieties to the  $\text{Zn}^{\text{II}}$  center strongly support the proposed mechanism.

## 3. Conclusions

We have successfully exploited a novel *N*-Boc-*L*-proline-modified 1,8-naphthyridine fluorescent chemosensor **L** for the detection of  $\text{Zn}^{\text{II}}$  with high selectivity and sensitivity. The photophysical behaviors of **L** and **L**+ $\text{Zn}^{\text{II}}$  coordinated complexes were characterized with a combined experimental and computational study. The remarkable fluorescence enhancement was attributed to the complexation of **L** with  $\text{Zn}^{\text{II}}$ . The competition experiments showed that the fluorescence response of **L** for



Zn<sup>II</sup> was not affected by the presence of other metal ions. In addition to the fluorescence titration and the Job's plot analyses, the binding events of **L** with Zn<sup>II</sup> was confirmed as 1:1 with a high binding constant value of  $5.94 \times 10^4 \text{ M}^{-1}$  and a detection limit of  $3.4 \times 10^{-6} \text{ M}$ . A new concept based on the 1,8-naphthyridine molecular scaffold could be explored for the simple detection of metal ions and specific Zn<sup>II</sup>-selective chemosensors for potential applications in environmental, biological, and medical areas.

## Experimental Section

### Materials and Instrumentation

All reagents and solvents in the experiments were commercial and used without further purification, unless stated otherwise. All solutions of metal ions were in their chloride or nitrate salts (Li<sup>I</sup>, K<sup>I</sup>, Mn<sup>II</sup>, Mg<sup>II</sup>, Cu<sup>II</sup>, Zn<sup>II</sup>, Cd<sup>II</sup>, Pb<sup>II</sup>, Fe<sup>II</sup>, Fe<sup>III</sup>, Cr<sup>III</sup>, Ni<sup>II</sup>, Ag<sup>I</sup>, and Co<sup>II</sup> as a chloride; Hg<sup>II</sup> as a nitrate).

Silica gel 60 (200–300 mesh) was used for flash chromatography. Merck silica gel plates (60F-254) were used for thin layer chromatography (TLC). 1,8-Naphthyridine ligands (**L**) were prepared by using a modified method, according to the literature procedure.<sup>[15]</sup>

<sup>1</sup>H and <sup>13</sup>C NMR spectra were recorded on a Bruker Avance 500 spectrometer, Tetramethylsilane was an internal standard. IR spectroscopy was measured on a Nicolet 170SX FT-IR spectrophotometer. HRMS was measured on Waters Xevo G2-XS QToF. UV/Vis absorption spectra were obtained on a Hitachi U-3010 spectrometer. Fluorescence emission spectra were recorded by using a Hitachi F-7000 fluorescence spectrometer.

DFT calculations at the B3LYP/6-31G\* and 6-31G\* + LanI2dz level were carried out using the Gaussian 09 program package.<sup>[16]</sup> Frequency analysis was further carried out to confirm that the structures obtained are really minimal.

### Synthesis of tert-Butyl 2-(5,7-dimethyl-1,8-naphthyridin-2-yl-carbamoyl)-pyrrolidine-1-carboxylate (**L**)

Ethyl chloroformate (0.220 mL, 0.232 mmol) was added dropwise to a 50 mL distilled THF solution of triethylamine (0.320 mL, 2.32 mmol) and *N*-Boc-L-proline (0.50 g, 2.32 mmol) at 0 °C. The mixture was continuously stirred at room temperature for 30 min. 2-Amino-5,7-dimethyl-1,8-naphthyridine (0.368 g, 2.20 mmol) was dissolved in dry THF (50 mL), and was then added to the above solution. After further vigorous stirring at room temperature for 24 h, the solution was treated with 30 mL ice water and extracted with 3 × 30 mL of ethyl acetate. The volatiles were concentrated under vacuum and subjected to column chromatography to obtain a white solid (ethyl acetate/methanol = 70/1). Yield: 74%; mp = (162–163) °C; <sup>1</sup>H NMR (500 MHz, CDCl<sub>3</sub>) δ = 8.91 (d, *J* = 16 Hz, 1H), 8.51 (d, *J* = 10 Hz, 1H), 8.33 (s, 1H), 7.15 (s, 1H), 4.3 (d, *J* = 9.5 Hz, 1H), 3.54 (d, *J* = 7.0 Hz, 2H), 2.72 (s, 3H), 2.67 (s, 3H), 1.95–2.01 (m, 4H), 1.39–1.50 ppm (m, 9H). <sup>13</sup>C NMR (126 MHz, CDCl<sub>3</sub>) δ = 172.40, 171.46, 162.96, 155.56, 154.42, 152.58, 145.17, 135.48, 122.23, 118.64, 113.48, 80.83, 77.41, 77.15, 76.90, 62.00, 60.30, 47.52, 31.43, 28.30, 25.40, 24.55, 23.90, 20.97, 17.96, 14.13 ppm. IR (KBr): 3462, 2976, 2929, 1696, 1604, 1513, 1405, 1312, 1281, 1167, 1089, 893, 805, 772. Calcd. for C<sub>20</sub>H<sub>26</sub>N<sub>4</sub>O<sub>3</sub>: C, 64.84; H, 7.07; N, 15.12. Found: C, 63.54; H, 7.18; N, 14.97. ESI HRMS *m/z* [*M*+H]<sup>+</sup>: 371.45 g mol<sup>-1</sup>. Exact Mass: 370.20 g mol<sup>-1</sup>.

### Synthesis of *N*-(5,7-Dimethyl-1,8-naphthyridin-2-yl)pyrrolidine-2-carboxamide (UNBoc-L)

Trifluoroacetic acid (228 mg, 2.0 mmol) was added to a 30 mL CH<sub>2</sub>Cl<sub>2</sub> solution of **L** (270 mg, 1.0 mmol) at 0 °C. After stirring at room temperature for 2 h, the solution was treated with 20 mL ice water and extracted with 3 × 20 mL of CH<sub>2</sub>Cl<sub>2</sub>. The organic solvents were concentrated under vacuum and subjected to column chromatography to obtain a light yellow solid (ethyl acetate/methanol = 80/1). Yield: 90%; mp = (150–152) °C; <sup>1</sup>H NMR (500 MHz, CDCl<sub>3</sub>) δ = 10.62 (s, 1H), 8.47 (d, *J* = 8.4 Hz, 1H), 8.27 (d, *J* = 8.27 Hz, 1H), 7.08 (s, 1H), 3.92 (dd, *J* = 9.3, 3.91 Hz, 1H), 3.00–3.09 (m, 2H), 2.67 (s, 3H), 2.62 (s, 3H), 2.17–2.25 (m, 2H), 2.02–2.07 (m, 1H), 1.77–1.73 ppm (m, 2H). <sup>13</sup>C NMR (126 MHz, CDCl<sub>3</sub>) δ = 172.40, 171.46, 162.96, 155.56, 154.42, 152.58, 145.17, 135.48, 122.23, 118.64, 113.48, 80.83, 77.41, 77.15, 76.90, 62.00, 60.30, 47.52, 31.43, 28.30, 25.40, 24.55, 23.90, 20.97, 17.96, 14.13 ppm. IR (KBr): 3462, 2976, 2929, 1696, 1604, 1513, 1405, 1312, 1281, 1167, 1089, 893, 805, 772. Calcd. for C<sub>15</sub>H<sub>18</sub>N<sub>4</sub>O: C, 66.64; H, 6.71; N, 20.73. Found: C, 66.58; H, 6.77; N, 20.70. ESI HRMS *m/z* [*M*+H]<sup>+</sup>: 271.21 g mol<sup>-1</sup>. Exact Mass: 270.15 g mol<sup>-1</sup>.

## Acknowledgements

This work was supported by the Natural Science Foundation of Sichuan Provincial Department of Education (17ZA0330).

## Conflict of Interest

The authors declare no conflict of interest.

**Keywords:** 1,8-naphthyridine • chelation mechanism • chemosensors • fluorescence emission • Zn<sup>II</sup> detection

- [1] a) R. W. Sinkeldam, N. J. Greco, Y. Tor, *Chem. Rev.* **2010**, *110*, 2579–2619; b) Z. Xu, Y. Yoon, D. R. Spring, *Chem. Soc. Rev.* **2010**, *39*, 1996–2006; c) J. F. Zhang, Y. Zhou, J. Yoon, *Chem. Soc. Rev.* **2011**, *7*, 3416–3429; d) J. L. Kolanowski, F. Liu, *Chem. Soc. Rev.* **2018**, *47*, 195–208; e) D. Wu, A. C. Sedgwick, T. Gunnlaugsson, E. U. Akkaya, J. Yoon, T. D. James, *Chem. Soc. Rev.* **2017**, *46*, 7105–7123.
- [2] a) H. Kim, J. Kang, K. B. Kim, E. J. Song, C. Kim, *Spectrochim. Acta Part A* **2014**, *118*, 883–887; b) H. F. Qian, T. Tao, Y. H. Wang, G. Yin, W. Huang, *Inorg. Chem. Commun.* **2015**, *58*, 99–102; c) H. Su, X. Chen, W. Fang, *Anal. Chem.* **2014**, *86*, 891–899.
- [3] a) Z. Li, L. Zhang, L. Y. Wang, L. Cai, M. Yu, L. Wei, *Chem. Commun.* **2011**, *47*, 5798–5800; b) Y. S. Kim, G. J. Park, J. J. Lee, S. Y. Lee, C. Kim, *RSC Adv.* **2015**, *5*, 11229–11239; c) T. A. Khan, M. Sheoran, M. V. N. Raj, S. Jain, D. Gupta, S. G. Naik, *Spectrochim. Acta Part A* **2018**, *189*, 176–182; d) N. Roy, A. Dutta, P. Mondal, P. C. Paul, T. S. Singh, *J. Fluoresc.* **2017**, *27*, 1307–1321; e) R. Borthaku, U. Thapa, M. Asthana, S. Mitra, K. Ismail, R. A. Lal, *J. Photochem. Photobiol. A* **2015**, *301*, 6–13; f) L. A. Finney, T. V. O'Halloran, *Science* **2003**, *300*, 931–936.
- [4] T. V. O'Halloran, *Science* **1993**, *261*, 715–725.
- [5] a) M. P. Cuajungco, G. Lees, *J. Neurobiol. Dis.* **1997**, *4*, 137–169; b) K. H. Falchuk, *Mol. Cell. Biochem.* **1998**, *188*, 41–48.
- [6] a) A. Avci, I. Kay, *Tetrahedron Lett.* **2015**, *56*, 1820–1824; b) J. Ma, R. Sheng, J. Wu, W. Liu, H. Zhang, *Sens. Actuators B* **2014**, *197*, 364–369; c) N. Li, Y. Ma, S. Zeng, Y. Liu, X. Sun, Z. Xing, *Synth. Met.* **2017**, *232*, 17–24; d) P. Kaur, R. Singh, V. Kaur, D. Talwar, *Sens. Actuators B* **2018**, *254*, 533–541; e) W. Wu, P. Mao, Y. Wang, X. Zhao, Z. Xu, Y. Xue, *Spectrochim. Acta Part A* **2018**, *188*, 324–331; f) P. Azadbakht, M. Koolivand, J. Khanabadi, *Anal. Methods* **2017**, *9*, 4688–4694; g) S. Lohar, S. Pal, M. Mukherjee, A. Maji, N. Demitri, P. Chattopadhyay, *RSC Adv.* **2017**, *7*, 25528–25534.

- [7] a) X. Liu, N. Zhang, J. Zhou, T. Chang, C. Fang, D. Shanguan, *Analyst* **2013**, *138*, 901–906; b) N. J. Williams, W. Gan, J. H. Reibenspies, R. D. Hancock, *Inorg. Chem.* **2009**, *48*, 1407–1415; c) J. Wang, W. Lin, W. Li, *Chem. Eur. J.* **2012**, *18*, 13629–13632.
- [8] a) S. H. Lu, R. Shang, J. M. Fang, *Org. Lett.* **2016**, *18*, 1724–1727; b) L. Fu, X. Feng, J. J. Wang, Z. Xun, J. D. Hu, J. J. Zhang, Y. W. Zhao, Z. B. Huang, D. Q. Shi, *ACS Comb. Sci.* **2015**, *17*, 24–31; c) Z. Li, X. Lv, Y. Chen, W. Fu, *Dyes Pigm.* **2014**, *105*, 157–162; d) M. Du, C. Hu, L. Wang, C. Li, Y. Han, X. Gan, Y. Chen, W. Mu, M. L. Huang, W. Fu, *Dalton Trans.* **2014**, *43*, 13924–13931; e) A. K. Mahapatra, G. Hazra, N. K. Das, P. Sahoo, S. Goswami, H. K. Fun, *J. Photochem. Photobiol. A* **2011**, *222*, 47–51; f) A. Goel, P. Nag, S. Umar, *Synlett* **2014**, *25*, 1542–1546; g) S. Umar, A. K. Jha, D. Purohit, A. Goel, *J. Org. Chem.* **2017**, *82*, 4766–4773; h) X. Zhang, R. Wang, C. Fan, G. Liu, S. Pu, *Dyes Pigm.* **2017**, *139*, 208–217; i) D. Yao, X. Huang, F. Guo, P. Xie, *Sens. Actuators B* **2018**, *256*, 276–281.
- [9] a) Z. Li, W. Zhao, X. Li, Y. Zhu, C. Liu, L. Wang, M. Yu, L. Wei, M. Tang, H. Zhang, *Inorg. Chem.* **2012**, *51*, 12444–12449; b) S. Dey, D. Sain, S. Goswami, *RSC Adv.* **2014**, *4*, 428–433.
- [10] a) D. Ma, Q. Cai, *Acc. Chem. Res.* **2008**, *41*, 1450–1460; b) R. Laura, H. Konrad, B. Alfons, M. Fabian, *J. Am. Chem. Soc.* **2015**, *137*, 12121–12130; c) D. Bhattacharjee, B. Kshira, B. Myrboh, *RSC Adv.* **2016**, *6*, 95944–95950.
- [11] a) Y. Dong, R. Fan, W. Chen, P. Wang, Y. Yang, *Dalton Trans.* **2017**, *46*, 6769–6775; b) M. Amirnasr, R. S. Erami, S. Meghdadi, *Sens. Actuators B* **2016**, *233*, 355–360.
- [12] J. Qin, Z. Yang, *J. Photochem. Photobiol. A* **2016**, *324*, 152–158.
- [13] S. X. Luo, V. Tiwow, M. Maeder, G. A. Lawrance, *J. Coord. Chem.* **2010**, *63*, 2400–2418.
- [14] a) N. Roy, H. A. R. Pramanik, P. C. Paul, T. S. Singh, *Spectrochim. Acta Part A* **2015**, *140*, 150–155; b) A. Ding, F. Tang, T. Wang, X. Tao, J. Yang, *J. Chem. Sci.* **2015**, *127*, 375–382.
- [15] M. L. Clarke, J. A. Fuentes, *Angew. Chem. Int. Ed.* **2007**, *46*, 930–933; *Angew. Chem.* **2007**, *119*, 948–951.
- [16] M. J. Frisch, G. W. Trucks, H. B. Schlegel, et al. 2004. Gaussian 09, revision D.01, Gaussian, Inc. Wallingford CT.

---

Received: May 8, 2018